

Comparison between NIST Graphene and AIST GaAs Quantized Hall Devices

Takehiko Oe, *Member, IEEE*, Albert F. Rigosi, Mattias Kruskopf, Bi-Yi Wu, Hsin-Yen Lee, Yanfei Yang, Randolph E. Elmquist, *Senior Member, IEEE*, Nobu-hisa Kaneko, *Member, IEEE*, Dean G. Jarrett*, *Senior Member, IEEE*

Abstract—Several graphene quantized Hall resistance (QHR) devices manufactured at the National Institute of Standards and Technology (NIST) were compared to GaAs QHR devices and a 100 Ω standard resistor at the National Institute for Advanced Industrial Science and Technology (AIST). Measurements of the 100 Ω resistor with the graphene QHR devices agreed within 5 n Ω/Ω of the values for the 100 Ω resistor obtained through GaAs measurements. The electron density of the graphene devices was adjusted at AIST to restore device properties such that operation was possible at low magnetic flux densities of 4 T to 6 T. This adjustment was accomplished with a functionalization method utilized at NIST, allowing for consistent tunability of the graphene QHR devices with simple annealing. Such a method replaces older and less predictable methods for adjusting graphene for metrological suitability. The milestone results demonstrate the ease with which graphene can be used to make resistance comparison measurements among many National Metrology Institutes.

Index Terms— quantized Hall resistance, epitaxial graphene, cryogenic current comparator, electron density, standard resistor

I. INTRODUCTION

THE development of graphene-based quantized Hall resistance (QHR) standards [1] over the past decade has provided an avenue for proliferation of quantum standards beyond National Metrology Institutes (NMIs) and several primary standards laboratories [2]. For ease of use and implementation, it is essential that graphene devices exhibit a tunable electron density in air. Historically, the storage of devices in an inert gas (argon) environment at the National

Institute of Standards and Technology (NIST) has been able to promote electron density stability in graphene devices. However, the problem of stability in ambient laboratory conditions remained an issue, warranting the pursuit of techniques to treat graphene devices such that they may exhibit stability in ambient air. Only then would international comparisons between devices be more easily viable.

To demonstrate the success of air-stable graphene devices, comparisons were made between NIST epitaxial graphene (EG) QHR devices and gallium arsenide (GaAs) QHR devices from the National Institute for Advanced Industrial Science and Technology (AIST) with accuracies of less than 5 n Ω/Ω . The comparison took place over a two-year period with one of the devices (N05) making two round-trips from NIST to AIST.

An older method for adjusting the electron density, namely the use of nitric acid vapors, was used initially for two devices (only one of which, N05, is shown) as a basis for assessment of the new method, functionalization of the EG surface with chromium tricarbonyl ($\text{Cr}(\text{CO})_3$) [3]. All devices were also used to determine the deviations of a 100 Ω resistor at AIST, and combined with similar data using the GaAs QHR devices, a complete set of consistency checks were obtained [4]. This paper is an extension of the corresponding proceedings paper and makes use of similar language [4] and further elaborates on one (N05) of the two devices previously reported.

II. GRAPHENE GROWTH

EG growth is performed on the Si-face of silicon carbide (SiC) and involves the sublimation of Si atoms at high temperatures. The surface becomes enriched with carbon atoms that form a honeycomb lattice. Square SiC substrates diced from on-axis 4H-SiC(0001) semi-insulating wafers were used. The EG was grown using a combination of face-to-graphite orientation and polymer-assisted-sublimation growth (PASG) [5]. Temperatures reach a maximum of 1900 $^\circ\text{C}$ in an argon atmosphere with the SiC (0001) facing a polished disk of glassy carbon. All EG devices were processed in the same graphite-lined resistive-element furnace, with the chamber first flushed with argon gas and filled with 100 kPa argon from a 99.999 % liquid argon source. Epitaxial growth occurs with heating and cooling rates of approximately 1.5 K/s and about 270 s annealing time at approximately 1900 $^\circ\text{C}$.

The graphene-based devices are prepared by similar

Manuscript received April 16, 2019; revised XX. For a subset of the author list, this work was prepared as part of their official duties for the U. S. Government. *Asterisk indicates corresponding author.*

T. Oe and N. Kaneko are with the National Metrology Institute of Japan, National Institute of Advanced Industrial Science and Technology, Tsukuba 305-8563, Japan (email: t.oe@aist.go.jp and nobuhisa.kaneko@aist.go.jp).

A. F. Rigosi, R. E. Elmquist, and D. G. Jarrett are with the National Institute of Standards and Technology, Gaithersburg, MD 20899, USA (e-mails: afr@nist.gov, dean.jarrett@nist.gov, and randolph.elmquist@nist.gov).

M. Kruskopf and Y. Yang are with the University of Maryland, Joint Quantum Institute, College Park, MD 20742, USA (email: mattias.kruskopf@nist.gov, yanfei.yang@gmail.com).

B.-Y. Wu is with the Graduate Institute of Applied Physics, National Taiwan University, Taipei 10617, Taiwan (email not available).

H.-Y. Lee is with Theiss Research, La Jolla, CA 92037, USA (email: hylai@gmail.com).

methods described rigorously in other work [6] – [8]. During device fabrication, the EG is protected by a layer of Pd-Au and later etched into a Hall bar geometry. Following the deposition of electrical contacts using photolithography, the EG device is functionalized with $\text{Cr}(\text{CO})_3$ and then mounted onto a transistor outline (TO-8) package [3]. Two devices from previous work and first used in the comparison were processed without $\text{Cr}(\text{CO})_3$ for initial measurements (mid-2017) to demonstrate how the electron density can be adjusted with exposure to nitric acid vapor [4]. During the interim, the functionalization process was optimized so that measurements after 2017 could utilize a set of EG devices with easily adjustable electron densities (of which N05 was a member).

III. MEASUREMENT SYSTEM AND INITIAL GRAPHENE MEASUREMENT

Prior to travel, several EG QHR devices were characterized at NIST and found to exhibit an onset of the $i = 2$ plateau ($R_K/2 \approx 12906.4037 \Omega$) at magnetic flux densities (B -fields) within 3 T and 6 T. After characterization, the EG QHR devices were then remounted onto TO-8 packages and were stored in a small vacuum canister backfilled with argon as an extra protective measure. The transport canister consisted of a metal-glass-metal tube of diameter 2.54 cm and length of 7.62 cm with KF-25 flanges on the ends. The tube provided a transparent window if necessary for inspection during travel.

At AIST, the devices were stored in the sealed transport canister until prepared for measurement. EG devices were placed in a dual sample probe for initial characterization. Two devices (N05, G19 [4]) were then cooled to about 0.5 K using a ^3He wet refrigerator with a 15 T superconducting magnet for precision measurements, whereas the more recent D-series devices (D1, D2, D3), as well as N05 post-functionalization [4], were cooled with a cryogen-free, closed-loop, dilution refrigerator. B -fields up to 12 T were adequate for the EG and GaAs devices.

A cryogenic current comparator (CCC) bridge, similar to the system described in reference [9], was used for these measurements. For the comparison of these devices with a 100Ω standard resistor, a winding ratio of 2065:16 was used. For the 1:1 comparison of QHR devices, 2065:2065 was used. In these comparisons, the balanced voltages were about 0.27 V and 0.35 V, respectively. During the initial testing, the EG device without $\text{Cr}(\text{CO})_3$ treatment exhibited higher electron densities, requiring a higher B -field of at least 10 T for the device to be quantized. The electron density was then adjusted at AIST, either with nitric acid vapor or a combination of functionalization and basic annealing, as described in the next sections for use at lower B -fields.

IV. GRAPHENE ADJUSTMENT AND CHARACTERIZATION

Historically, there have been several methods of adjusting EG devices, all with various advantages and disadvantages [10–14]. In our case, the effectiveness of functionalization was highlighted by comparing it to the method of adjustment via exposure to nitric acid vapors. The black curves in Fig. 1

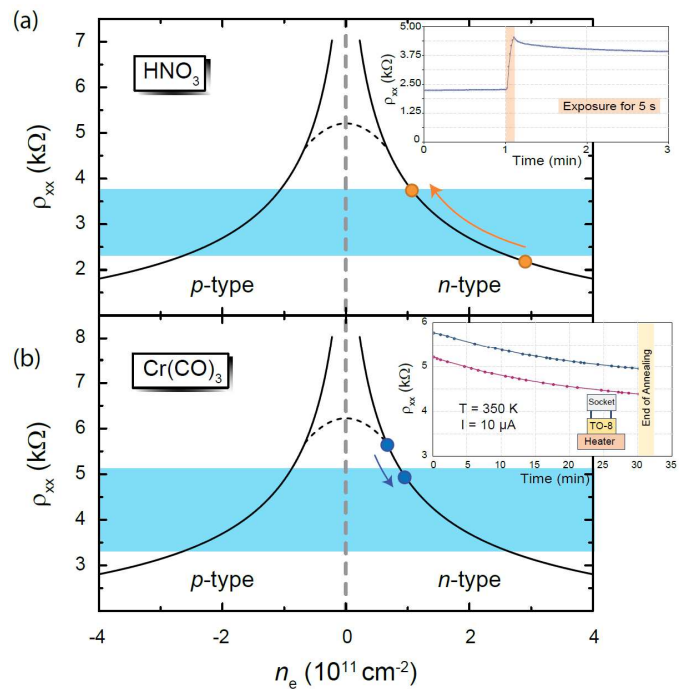


Fig. 1. The relationship between n_e and ρ_{xx} at room temperature is shown, with the dotted line representing the realistic transition between hole-dominated (p -type) or electron-dominated (n -type) graphene. (a) The first method is nitric acid vapor exposure, which causes n_e to drop suddenly within seconds (and ρ_{xx} to increase suddenly), as indicated by the orange dot approaching the Dirac point of graphene. Inset shows time-dependent monitoring of ρ_{xx} . (b) Functionalizing EG with $\text{Cr}(\text{CO})_3$ sets devices with an inherently lower n_e , as indicated by the blue dot. With a simple, timed anneal on the order of 30 min, this method is more reliable and predictable than nitric acid treatment. Furthermore, it can be reset and readjusted with ease [3]. The inset shows two curves: the top blue curve is the monitored ρ_{xx} as that same device is subjected to the 350 K annealing whereas the bottom magenta is an example of a different device being monitored and annealed in the same way. The regions in light blue represent the range of n_e that would enable lower B -field access to the QHR.

represent typical relationships between the electron density (n_e) and the longitudinal resistivity (ρ_{xx}). The dotted black curve near charge neutrality reflects the phenomenon of electrons and holes both existing within the device as it transitions from one charge polarity to another. If n_e is too low (less than 10^{11} cm^{-2}), the $i = 2$ Hall plateau begins to lose its flatness, rendering it useless for resistance metrology.

In Fig. 1 (a), the effect on n_e from exposing a device to nitric acid vapors is illustrated. Methods for treating the EG devices prior to measurement allow for easier access to the $i = 2$ plateau ($B < 6$ T). The EG device, whose low initially-low longitudinal resistivity (orange dot) corresponded to the higher B -field requirement (approximately 10 T for the onset of $i = 2$ plateau), had n_e drop drastically after approximately 5 s of vapor exposure. Such determinations of n_e can be made when ρ_{xx} is monitored at room temperature. This information is provided in the inset, with the 5 s exposure causing an increase in ρ_{xx} . The problem with this method is that it is not entirely controllable and requires a facility for safe handling of hazardous materials. The lack of control results in devices which are easily over-adjusted, requiring further processing to bring them to a useful range. In this case, the nitric acid did

not cause an overshoot in the desired n_e , but rather, landed just within the range of a useful n_e (shown as light blue on Fig. 1), where the “range of usefulness” indicates reliable access to the QHR with lower B -fields (between 4 T and 6 T).

In Fig. 1 (b), a similar effect on n_e is shown as a result of simply annealing the device at 350 K for 30 min. Though the process is slower than in (a), it is more controllable, allowing for a finer selection of desired n_e . Furthermore, the principles of functionalization and adsorption ensure that the process for obtaining, resetting, and making new adjustments to n_e are reproducible, reliable, and safer than methods like nitric acid vapor exposure.

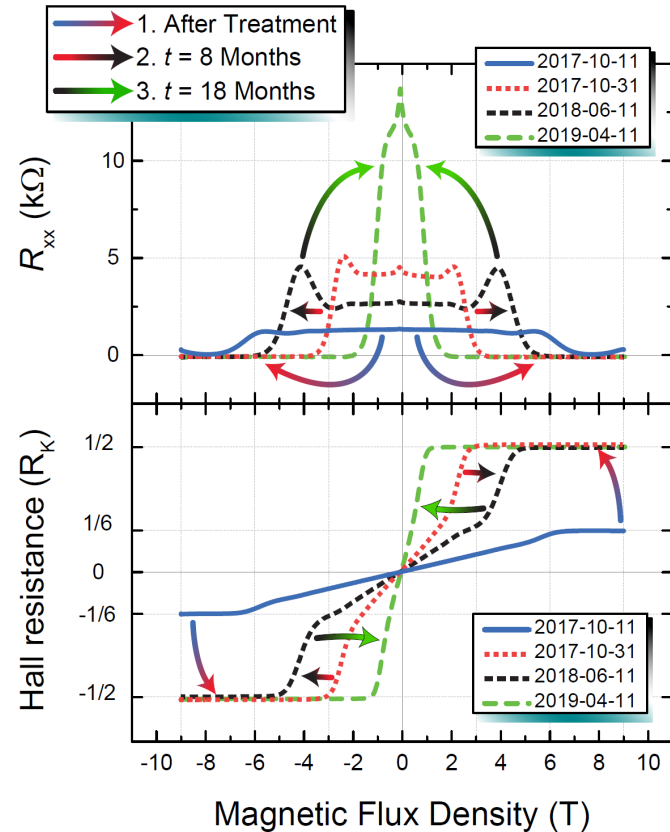


Fig. 2. The top and bottom panels show the longitudinal and Hall resistances, respectively, of an older device (N05). Red (short-dotted) and black (short-dashed) curves were measured after functionalization of EG (using $\text{Cr}(\text{CO})_3$ as the stabilizing agent). After the initial blue (solid) curve showing an unusable QHR (due to the device being stored in air), n_e remains stable and between approximately $1 \times 10^{11} \text{ cm}^{-2}$ and $3.5 \times 10^{11} \text{ cm}^{-2}$ for periods of at least 18 months. The green, long-dashed curve was obtained 18 months after the initial measurement.

A graphical representation of the advantages of using $\text{Cr}(\text{CO})_3$ as a stabilizing agent is presented in Fig. 2. The top and bottom panels show the longitudinal and Hall resistances, respectively, measured for the device labeled as N05 over a period of 18 months. N05 initially underwent nitric acid treatment due to its high n_e (greater than 10^{12} cm^{-2}). Starting in late 2017 (after the date of the blue curve), and after the return of N05 to NIST, all devices underwent semi-permanent functionalization, enabling an immediate stabilization of n_e to

lower values on the order of 10^{11} cm^{-2} (blue curve converting to red within 1 day). As long as the device was stored in an ambient laboratory environment, n_e remained stable for low- B -field access. Over the 18-month period, the device exhibited shifting in n_e between approximately $1 \times 10^{11} \text{ cm}^{-2}$ and $3.5 \times 10^{11} \text{ cm}^{-2}$ for (red curve to black curve to green curve), evidently requiring the functionalization process to be further optimized, as described in Reference [3].

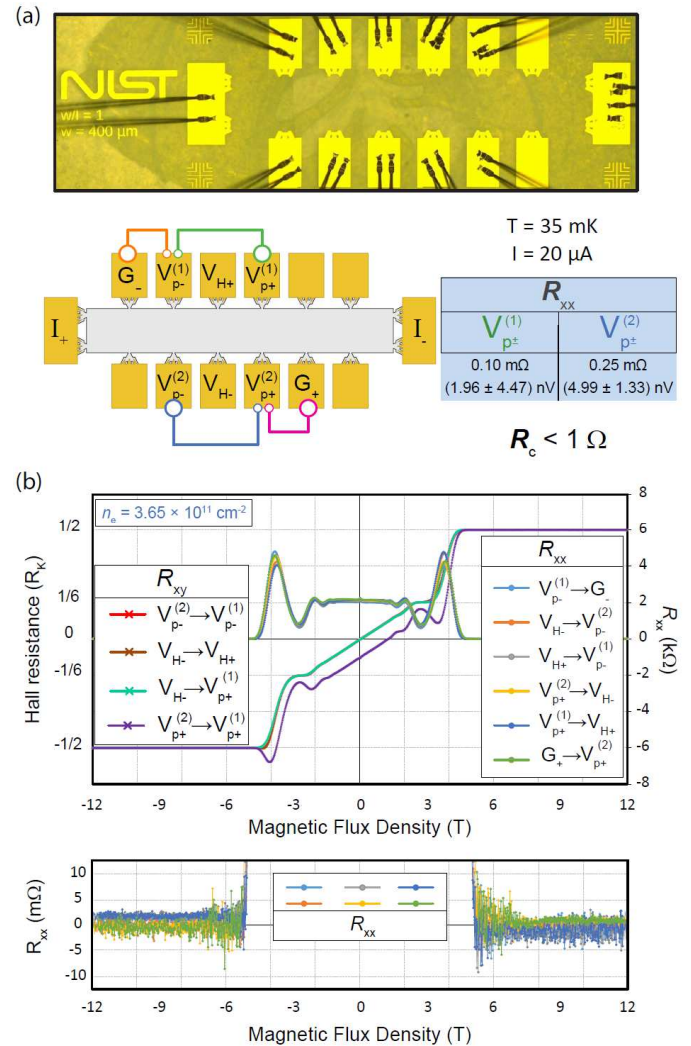


Fig. 3. (a) Optical image of an EG device is shown along with an illustration of the precision measurements done after annealing. The numbers listed for an example device (D3 at 11 T) offer insight on the high quality of the QHR. Green and blue lines indicate the sides of the device at which ρ_{xx} is measured, with corresponding orange and pink lines for ground, respectively. All contact resistances in this case are below 1Ω . (b) Hall and longitudinal voltage measurements are performed after basic annealing for functionalized devices and converted to resistances. The slope of R_{xy} is used at small B -fields to obtain n_e . The longitudinal resistance is magnified to highlight excellent EG device quantization.

By using the procedure developed at NIST, n_e was lowered to restore the device properties so operation at lower B -fields was possible [15, 16]. The annealing procedure was applied to all functionalized devices, lowering the required B -field for the $i = 2$ plateau onset from 10 T to 5 T. One device’s characterization is summarized in Fig. 3. The typical device

Hall bar geometry is imaged in Fig. 3 (a) accompanied by an illustration of the characterization measurement. The top and bottom sides of the EG device have their ρ_{xx} measured at 12 T, with both being below 0.3 m Ω at 35 mK and 20 μ A. For that device, all contact resistances were measured to be under 1 Ω .

Fig. 3 (b) shows the Hall and longitudinal resistance measurements that verify the quality of the EG device. The example device shown started out with a low n_e (due to functionalization) and was systematically annealed to obtain a plateau onset at lower B -fields. One main indication of excellent quantization comes from the measurement of the longitudinal resistance along the sides of the EG device, which should be at the same electric potential. The longitudinal resistances are less than 5 m Ω , indicating high-quality quantization.

V. COMPARISON BETWEEN GRAPHENE, GAAS, AND A STANDARD RESISTOR

A. Comparing Against a 100 Ω Resistor

Initial measurements against a 100 Ω resistor were made using two EG devices [4], one of which was originally not functionalized (N05, represented by orange squares in Fig. 4, mid-2017), and yielded a difference of 4.4 n Ω/Ω . Measurements on the second early device (G19 [4]) also agreed. The N05 result agreed with the predicted value for that resistor, as shown in Fig 4, within the expanded uncertainty ($k = 2$) of 24 n Ω/Ω . The applied B -field for that measurement was 12.0 T. The graphene device for this measurement (N05) had its longitudinal resistance measured with a simple voltmeter without current reversal, yielding a quick upper bound of 0.1 m Ω . Contact resistances of less than 0.3 Ω were also measured using the 3-terminal method.

Fig. 4 shows the long-term behavior of AIST’s SR102 100 Ω resistor, primarily through the measurements made against several GaAs QHR devices from NMIJ. NIST EG devices are represented as orange and blue squares, with the former indicating the N05 device which underwent functionalization treatment after its first measurements in mid-2017. All newer NIST EG devices were labelled as the D-series and were functionalized after growth to stabilize n_e for future use. The Type A uncertainties for the D-series devices ranged from 0.85 n Ω/Ω to 1.60 n Ω/Ω . The inset provides measurement clarity for the previous two years.

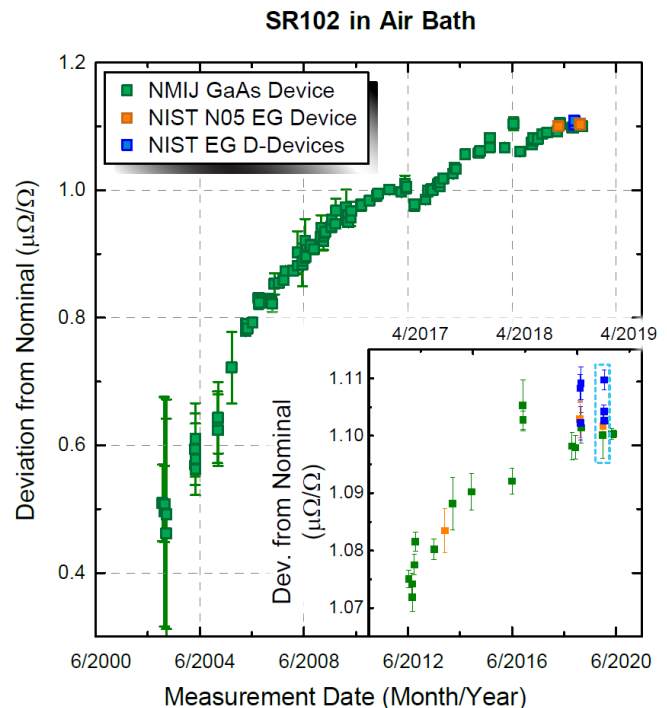


Fig. 4. Deviations from the nominal value of SR102, a 100 Ω resistor at AIST, were measured by the GaAs device from NMIJ over the span of 16 years (green squares). Orange squares are used to track the N05 EG device from NIST which initially (2017) was not functionalized. N05 is reused after functionalization one year later. Blue squares represent the D-series EG devices from NIST. The inset provides a clear view of the measurements taken within the previous two years, with the dotted teal box indicating the measurements in Table I. All error bars indicate Type A uncertainties, which in many recent measurements, become smaller than the data points.

TABLE I
UNCERTAINTY MEASUREMENTS

Date	Device	Dev. From 100 Ω Nominal ($\mu\Omega/\Omega$)	Type A ($\mu\Omega/\Omega$)	Difference from GaAs ($\mu\Omega/\Omega$)
2019/01/18	GaAs	1.100 1	0.004 0	-
2019/01/19	N05	1.101 7	0.001 4	0.000 3
2019/01/21	D2	1.104 3	0.001 2	0.002 9
2019/01/22	D3	1.102 7	0.000 8	0.001 3
2019/01/23	D1	1.109 9	0.001 6	0.008 5
2019/01/24	GaAs	1.102 6	0.000 6	-

All QHR devices were measured in succession to obtain an overall summary of SR102’s deviations from nominal. The resulting numbers are shown in Table I. All of the measurements using EG QHR devices agreed with those obtained from the GaAs QHR device to within 5 n Ω/Ω . In the case of D1, the slightly larger value obtained can be ascribed to the abnormally high contact resistance present in two out of six contacts, with the values on the order of 100 Ω . A graphical representation of these data is presented in Fig. 5, with the blue points representing the GaAs QHR devices and the gray points representing all NIST EG QHR devices. The error bars indicate Type A uncertainties only. The Type B uncertainties are 1.5 n Ω/Ω .

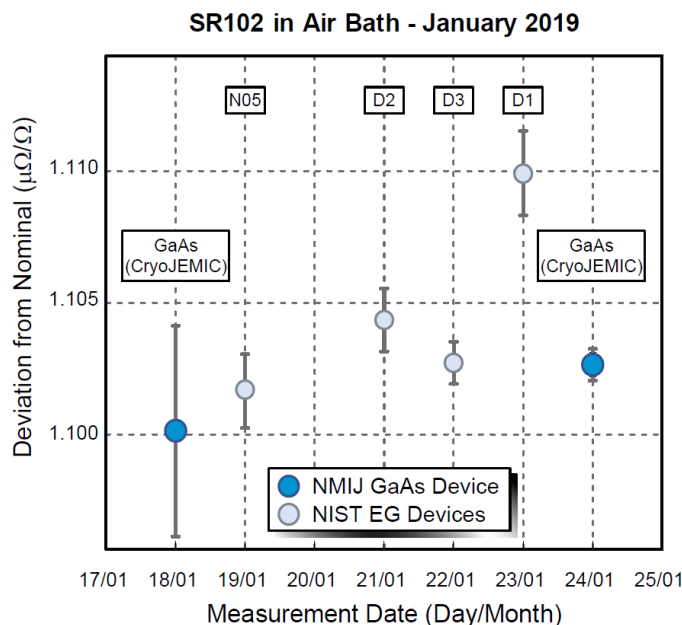


Fig. 5. All QHR devices' measurements against the SR102 resistor are compared here to show the agreement within $5 \text{ n}\Omega/\Omega$. D1 is slightly offset due to the contact resistance present in that device, as described in the main text. Blue and gray points represent the GaAs QHR and the NIST QHR devices, respectively. The error bars show the Type A uncertainties.

The compared QHR devices in Fig. 5, with the exception of D1, which was affected more strongly by contact resistances, agree within the limitations of the measurement system and the stability of the resistor, which together present potential deviations of $5 \text{ n}\Omega/\Omega$.

B. Comparison Between QHR Devices

The direct comparison of the N05 EG QHR and GaAs in October 2018 showed an absolute difference of $1.8 \text{ n}\Omega/\Omega$ at 11.1 T and 35 mK. A later comparison of an example NIST EG D-series device (D2) was performed against the same CryoJEMIC GaAs QHR device in January 2019, resulting in an agreement of $3.7 \text{ n}\Omega/\Omega$. Such measurements provided three consistency checks to ensure the validity of the NIST EG device functionality.

VI. CONCLUSION

All EG QHR devices were used to determine the deviations of a 100Ω resistor at AIST, and combined with data obtained with GaAs QHR devices, self-consistent results were obtained. We have assessed those measurements as demonstrating the success of tunable EG devices for long-term shelf-life and demanding travel conditions. Provided those devices are properly functionalized, international comparisons will continue to become more easily viable. Comparisons were also made between NIST EG QHR devices and GaAs QHR devices from AIST with uncertainties of less than $5 \text{ n}\Omega/\Omega$.

ACKNOWLEDGMENT

H.-Y. L. would like to thank Theiss Research for the opportunity. The work of B.-Y.W. at NIST was made possible by Prof. C.-T. Liang of National Taiwan University.

REFERENCES

- [1] F. Delahaye, T. J. Witt, R. E. Elmquist, and R. F. Dziuba, "Comparison of Quantum Hall Effect Resistance Standards of the NIST and the BIPM," *Metrologia* 37, 173 – 176 (2000).
- [2] D. Drung, M. Gotz, E. Pesel, H. J. Barthelmeß, and C. Hinrichs, *IEEE Trans. Instrum. Meas.* 62, 2820 (2013).
- [3] A. F. Rigosi *et al.*, "Gateless and reversible Carrier density tunability in epitaxial graphene devices functionalized with chromium tricarbonyl," *Carbon N. Y.*, vol. 142, pp. 468–474, Feb. 2019.
- [4] D. G. Jarrett, T. Oe, R. E. Elmquist, N.-H. Kaneko, A. F. Rigosi, M. Kruskopf, B.-Y. Wu, H.-Y. Lee, and Y. Yang. Transport of NIST Graphene Quantized Hall Devices and Comparison with AIST Gallium-Arsenide Quantized Hall Devices. *IEEE CPEM Conf. Dig.* 2018.
- [5] M. Kruskopf, D. M. Pakdehi, K. Pierz, S. Wundrack, R. Stosch, T. Dziomba, M. Götz, J. Baringhaus, J. Aprojanz, C. Tegenkamp, J. Lidzba, T. Seyller, F. Hohls, F. J. Ahlers and H.W. Schumacher "Comeback of epitaxial graphene for electronics: large-area growth of bilayer-free graphene on SiC" *2D Mater.*, 3, 041002, 2016.
- [6] Y. Yang, L.-I. Huang, Y. Fukuyama, F.-H. Liu, M. A. Real, P. Barbara, C.-T. Liang, D. B. Newell, and R. E. Elmquist, "Low Carrier Density Epitaxial Graphene Devices on SiC," *Small*, 11, 1, 90 – 95, 2015.
- [7] A. F. Rigosi, C.-I. Liu, N. R. Glavin, Y. Yang, H. M. Hill, J. Hu, A. R. Hight Walker, C. A. Richter, R. E. Elmquist, and D. B. Newell, "Electrical Stabilization of Surface Resistivity in Epitaxial Graphene Systems by Amorphous Boron Nitride Encapsulation," *ACS Omega*, 2, 2326 – 2332, 2017.
- [8] Y. Yang, G. Cheng, P. Mende, I.G. Calizo, R.M. Feenstra, C. Chuang, C.-W. Liu, G. R. Jones, A. R. Hight Walker, and R. E. Elmquist, "Epitaxial Graphene Homogeneity and Quantum Hall Effect in Millimeter-Scale Devices," *Carbon* 115, 229, 2017.
- [9] J. Kinoshita, K. Inagaki, C. Yamanouchi, K. Yoshihiro, S. Kawaji, N. Nagashima, N. Kikuchi, and J.-I. Wakabayashi, "Self-Balancing Resistance Ratio Bridge Using a Cryogenic Current Comparator," *IEEE Trans. Instrum. Meas.*, Vol. 38, No. 2, pp. 290-292, April 1989.
- [10] S. Lara-Avila, K. Moth-Poulsen, R. Yakimova, T. Bjørnholm, V. Fal'ko, A. Tzalenchuk, S. Kubatkin. Non-Volatile Photochemical Gating of an Epitaxial Graphene/Polymer Heterostructure. *Adv. Mater.*, 23, 878-882, 2011.
- [11] A. Tzalenchuk, S. Lara-Avila, K. Cedergren, M. Syväjärvi, R. Yakimova, O. Kazakova, T.J. Janssen, K. Moth-Poulsen, T. Bjørnholm, S. Kopylov, V. Fal'ko. Engineering and metrology of epitaxial graphene. *Solid State Commun.*, 151, 1094-1099, 2011.
- [12] A. Lartsev, T. Yager, T. Bergsten, A. Tzalenchuk, T. M. Janssen, R. Yakimova, S. Lara-Avila, S. Kubatkin. Tuning carrier density across Dirac point in epitaxial graphene on SiC by corona discharge. *Appl. Phys. Lett.*, 105, 063106, 2014.
- [13] N. Fletcher, P. Gournay, B. Rolland, M. Götz, S. Novikov, N. Lebedeva, A. Satrapinski. Experimental study of carrier density tuning in epitaxial graphene QHR devices. *IEEE CPEM Conf. Dig.* 2016.
- [14] H. He, K. H. Kim, A. Danilov, D. Montemurro, L. Yu, Y. W. Park, F. Lombardi, T. Bauch, K. Moth-Poulsen, T. Iakimov, R. Yakimova. Uniform doping of graphene close to the Dirac point by polymer-assisted assembly of molecular dopants. *Nat. Commun.*, 9, 3-9, 2018.
- [15] A. F. Rigosi, A. R. Panna, S. U. Payagala, M. Kruskopf, M. E. Kraft, G. R. Jones, B.-Y. Wu, H.-Y. Lee, Y. Yang, J. Hu, D. G. Jarrett, D. B. Newell, and R. E. Elmquist. Graphene Devices for Table-Top and High Current Quantized Hall Resistance Standards. *IEEE Trans. Instrum. Meas.* 68, 1870-1878, 2019.
- [16] T. J. B. M. Janssen, S. Rozhko, I. Antonov, A. Tzalenchuk, J. M. Williams, Z. Melhem, H. He, S. Lara-Avila, S. Kubatkin, and R. Yakimova, "Operation of a Graphene quantum Hall resistance standard in cryogen-free table-top system," *2D Mater.*, 2, 035015, 1 – 9, 2015.



Takehiko Oe (M'06) was born in Kobe, Japan, in 1981. He received the B.E. degree in electrical engineering from the Kobe City College of Technology, Kobe, in 2004, the M.E. degree in electrical engineering from the Tokyo Institute of Technology, Tokyo, Japan, in 2006, and the Ph.D. degree in crystalline materials science from Nagoya University,

Nagoya, Japan, in 2015.

In 2006, he joined the National Metrology Institute of Japan, National Institute of Advanced Industrial Science and Technology, Tsukuba, where he was involved in the calibration service of dc resistance standards and the development of next-generation quantum dc resistance standards.



Albert F. Rigosi (M'17) was born in New York, NY, USA in 1989. He received the B.A., M.A., M.Phil., and Ph.D. degrees in physics from Columbia University, New York, NY, in 2011, 2013, 2014, and 2016, respectively.

From 2008 to 2015, he was a Research Assistant with the Columbia Nano Initiative. From 2015 to 2016, he was a Joint Visiting Research Scholar with the Department of Applied Physics of Stanford University in Stanford, CA, and the PULSE Institute of SLAC National Accelerator Laboratory in Menlo Park, CA. Since 2016, he has been a Physicist at the National Institute of Standards and Technology in Gaithersburg, MD. His research interests include two-dimensional electron systems and applications of those systems' behaviors for electrical metrology.

Dr. Rigosi is a member of the American Physical Society and the Mellon-Mays Initiative of The Andrew W. Mellon Foundation. He was awarded associateships and fellowships from the National Research Council (USA), the Optical Society of America, the Ford Foundation, and the National Science Foundation (Graduate Research Fellowship Program).



Mattias Kruskopf was born in Hamburg, Germany, in 1984. He received the M.Sc. degree in electronics engineering, with the focus on metrology, from the Bremen University of Applied Sciences, Bremen, Germany, in 2013. In 2017, he finished his Ph.D. research on epitaxial graphene for quantum resistance metrology in the working group of Low-dimensional

Electron Systems at the Physikalisch-Technische Bundesanstalt (PTB), Braunschweig, Germany.

In his current research at the National Institute of Standards and Technology (NIST), Gaithersburg, MD, he is focusing on improving the scalability and the adoption of graphene-based resistance standards.



Bi-Yi Wu received the B.S. degree in physics from National Cheng Kung University, Tainan, Taiwan, in 2013. He is currently pursuing the Ph.D. degree in Applied Physics at National Taiwan University, Taipei, Taiwan.

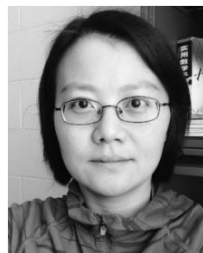
From Feb. 2016 to Aug. 2016, he was a visitor with the NS2 research group at the Université Paris-Sud, France. From Feb. 2017 to Jan. 2018, he was a guest researcher with NIST, MD. His research includes the electronic transport of CVD and epitaxial graphene at low temperatures and fabrication techniques for nanostructured devices.



Hsin-Yen Lee received the B.S. degree and the M.S. degree in physics from National Tsing Hua University, Hsinchu, Taiwan, in 2002 and 2004, and the Ph.D. degree in physics from National Taiwan University, Taipei, Taiwan, in 2012.

He fulfilled his mandatory Taiwanese military service in 2005. From 2006 to 2007, he was a senior Process Integration Engineer with the United Microelectronics Corporation, Hsinchu, Taiwan, and from 2012 to 2016, he was a Postdoctoral Researcher with the Institute of Atomic and Molecular Sciences, Academia Sinica, Taipei, Taiwan, and the Department of Physics, National Taiwan University, Taipei, Taiwan.

From 2016 to 2018, he had been a Guest Researcher with the National Institute of Standards and Technology (NIST) in Gaithersburg, MD. His research interest includes the development of surface treatment techniques on transparent semiconductor heterojunctions, the pursuit of graphene quantum Hall resistance standards, and the fabrication of graphene and other 2D material devices.

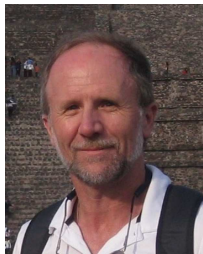


Yanfei Yang received the B.S. degree in applied optics from Sichuan University, Chengdu, China, in 1999 and the Ph.D. degree in physics from Georgetown University, Washington, DC, in 2010. Her Ph.D. thesis focused on quantum transport in carbon nanotubes and the investigation of possible intrinsic superconductivity in isolated carbon

nanotubes.

She was an Associate Researcher at the National Institute of Standards and Technology (NIST), Gaithersburg, MD, from 2012 to 2017, where she had been involved in the development of new resistance standards based on quantum Hall devices made of epitaxial graphene.

She was awarded the Physical Measurement Laboratory's (NIST) Distinguished Associated Award for advancing quantum metrology through the development of graphene quantum Hall resistance standards that offer robust, accurate, cost-effective dissemination of the ohm.



Randolph E. Elmquist (M'90–SM'98) received the Ph.D. degree in physics from the University of Virginia, Charlottesville, VA, in 1986. He leads the Quantum Conductance project at the NIST. Working for the past 32 years in the field of electrical and quantum metrology, he has contributed to the experimental design and measurement of

the electronic Kilogram and calculable impedance standards for the determination of the von Klitzing constant and alpha, the unitless fine structure constant. He leads the development of cryogenic current comparator systems, the quantum Hall effect, and graphene electronic devices for metrology.

Dr. Elmquist is a member of the American Physical Society.



Nobu-Hisa Kaneko (M'18) was born in Nagasaki, Japan, in 1967. He received the master's and Ph.D. degrees in condensed matter physics, with a focus on crystal growth of high-temperature superconducting materials and magnetic property of them by neutron scattering experiments, from Tohoku University, Sendai, Japan, in 1992 and 1997,

respectively.

From 1996 to 1999, he was with the National Research Institute in Inorganic Materials, Tsukuba, Japan. From 1999 to 2003, he was a Post-Doctoral Researcher with the Applied Physics Department, Stanford University, Stanford, CA, USA, where he was a Physicist with the Stanford Linear Accelerator Center (now the SLAC National Accelerator Laboratory). In 2003, he joined the National Metrology Institute of Japan, National Institute of Advanced Industrial Science and Technology (NMIJ/AIST), Tsukuba, Japan. He was involved in the development of programmable, pulse-driven ac Josephson voltage standards including the Johnson noise thermometry project, and single electron control project. Since 2003, he has been involved in the resistance calibration systems based on the quantum Hall effect. He is involved in condensed matter physics of strongly correlated electron systems. He is currently a Prime Senior Researcher and the Group Leader of the Applied Electrical Standards Group, NMIJ/AIST. His current research interests include condensed matter and material physics and their applications to metrology.



Dean G. Jarrett was (S'88–M'90–SM'99) was born in Baltimore, MD, in 1967. He received the B.S. degree in electrical engineering from the University of Maryland, College Park, in 1990 and the M.S. degrees in electrical engineering and applied biomedical engineering from Johns Hopkins University, Baltimore, in 1995 and 2008, respectively.

Since 1986, he has been with the National Institute of Standards and Technology (NIST), in Gaithersburg, MD, where he was a Cooperative Education Student from the University of Maryland. During this time, he worked in the DC resistance area on the automation of resistance calibration systems. In 1991 he joined NIST full time as an electrical engineer working on the development of an automated AC resistance calibration system and the development of new resistance standards. Since 1994, Mr. Jarrett has worked in the high resistance laboratory developing automated measurement systems and improved standard resistors to support high resistance calibration services and key comparisons. In recent years, Mr. Jarrett has worked on sensor technologies for the detection of biological molecules and low-current source and measure techniques. Since 2014, he has led the Metrology of the Ohm Project at NIST.